Chapter 5

Spatial and Temporal Development of Alternaria Blight Epidemics in Selected Sunflower Lines

Summary

The work reported in this chapter examined the development of artificially generated epidemics of *A. helianthi* in 9 sunflower lines grown at two field sites. The aim was to characterise the epidemics that developed in each line by calculating parameters that described disease spread in either space or time or both space and time. Parameters were evaluated primarily for their usefulness in differentiating quantitative resistance (QR), however they were also examined to detect aspects of epidemic development which may help further in the characterisation of QR or be useful for future decisions of experimental design and disease assessment methods. Disease severity ratings (DSRs), area under the disease progress curves (audpcs) and volumes beneath the plot of disease progress in space and time (GVs) were good indicators of QR, while apparent infection rates (r), disease gradients (b) and velocities of spread (v) were not. Three- dimensional surface plots of disease progress in both space and time allowed all epidemic parameters to be viewed simultaneously. DSRs taken prior to flowering were well correlated with DSRs taken at flowering and post-flowering. DSRs obtained for leaves in the low, middle and upper plant positions were poorly correlated.

5.1 Introduction

Temporal and spatial aspects of epidemic development are commonly used to evaluate partial or quantitative resistance to disease under field conditions. These aspects of epidemic analysis refer to the development of disease as a function of time, (temporal) and distance (spatial) from a point or line source. They are often described as disease progress and disease spread respectively. A reduction in either or both will slow the rate of epidemic development. Hence, measurements of disease progress and spread may provide ways of identifying sunflower lines that exhibit quantitative resistance (QR).

Disease progress curves are generated by plotting some measure of disease (incidence or severity) with time. Progress curves of polycyclic diseases are characteristically

sigmoidal in shape. Interpretation and comparison of such curves requires that curves are described by some numerical value. This usually involves linearisation of the progress curve so that the slope of the line can be easily calculated. This slope is then regarded as a measure of disease progress. Linearisation of the curve is achieved by using a suitable transformation model (Minogue, 1986). Disease progress is often expressed according to the method of Van der Plank (1963), where the apparent infection rate (r) of disease (y) increase in time (t), corrected for decreasing amounts of healthy tissue ($1-y$), is given by the formula:

$$r = 1/t_2-t_1 \ (\log_e y_2/1-y_2 - \log_e y_1/1-y_1)$$

where y = diseased tissue in the range $0<y<1$. More frequently, the equation is simplified to:

$$r = [\text{logit}\ (y_2) - \text{logit}\ (y_1)] \ / \ (t_2 - t_1)$$

where $\text{logit}\ (y) = \log_e\ (y\ /1-y)$. This method uses the logistic transformation model which may or may not be appropriate, depending on the nature of the "underlying distribution" (Kranz, 1974). By this, Kranz (1974) cautions that other transformations may be more appropriate for linearisation. For example, the logistic transformation is better suited to symmetrical or negatively skewed progress curves, whereas many progress curves are often asymmetrical and show a degree of positive skewness. Such disease progress curves are often better described by the Gompertz transformation which is itself positively skewed (Berger, 1981). The equation used for the gompertz transformation is given as:

$$\text{gompit}\ (y) = -\log_e\ (-\log_e y)$$

where y = diseased tissue in the range $0<y<1$. In some circumstances, the Gompertz model has been shown to give a better statistical fit than the logistic model (Berger and Luke, 1979; Luke and Berger, 1982; Hendrick and Pataky, 1988), while in others, the logistic model has been shown to give better estimates of disease progress (Jerger,

Jones and Griffiths, 1983; Jerger, 1983; Aylor and Ferrandino, 1988). In an examination of 113 epidemics, Berger (1981) found that the Gompertz transformation gave a better statistical fit than did the logistic transformation of disease progress data. Waggoner (1986) found that one or the other model gave a better fit depending on whether the epidemic "lags and then explodes or explodes then stagnates". Because there is no guarantee that any epidemic will follow one or the other model entirely, epidemiologists often apply more than one transformation model when analysing epidemics and choose that which gives the best fit. Although the Gompertz and logistic transformations are those most commonly applied, other transformations encountered include those of Bertalanffy, Mitscherlich and Weibull, as well as a monomolecular model. Of these, the Weibull model has gained some favour among epidemiologists because of its apparent ability to deal with both positive and negative skewness (Pennypacker *et al.*, 1980). However in practice, Waggoner (1986) doubts that the Weibull model has any "clear rationale", and despairs that at times, the proposed models fit or don't fit disease progress curves "with little or no rhyme or reason".

In recent years, the area under the disease progress curve (audpc) has become a popular method used to characterise disease progress. The trapezoidal rule is used to calculate the area under the plot of disease with time, and is given as:

$$\text{audpc} = \sum_{i=1}^{n} \left[(x_i + x_{i+1}) /2 \right] \left[t_{i+1} - t_i \right]$$

Where x_i and x_{i+1} are the proportion of leaf area infected at the ith and ith +1 observations respectively, t_i and t_{i+1} are the time (days) at the ith and ith +1 observations respectively and n is the total number of observations.

The audpc has some advantages over van der Plank's apparent infection rate. For example, audpc uses the actual data for disease intensity rather than estimates based on regression models, detects variations in rate that are obscured by the linearisation used to obtain *r* (Waggoner, 1986) and do not generate estimates biased by the asymptotes of the epidemic (Neher and Campbell, 1992). The audpc of different lines

can be easily analysed to detect relative levels of QR. In addition, audpc calculated at different time intevals during the epidemic may also provide information about the behaviour of resistance in relation to increasing disease pressure and susceptability of host tissue. Such details are lost when disease progress is reduced to a single parameter, as with van der Plank's apparent infection rate.

In order to gain more information than is offerred by *r*, Chakraborty *et al.* (1990) used a "broken stick" model to analyse the progress of anthracnose (*Colletotrichum gloeosporiodes* [Penz.] Penz. & Sacc in Penz.) epidemics in *Stylosanthes scabra.* They identified two distinct periods of epidemic development, 'early' and 'late', and modeled a straight line for each, ensuring that the lines for each period met at the time of transition from 'early' to 'late'. The slopes of the lines for each period gave better estimates of disease progress than the apparent infection rate.

The rate of spread of disease can be expressed as the gradient of the line connecting points of infection at various distances from a point or line source of inoculum (Gregory, 1968). Gradients can be calculated from both incidence and severity data and may be directly related to spore dispersal gradients. Disease gradients are plotted as $\log_e y$ versus $\log_e d$, where y and d are proportion of disease and distance from the inoculum source, respectively (Gregory, 1968). The rate at which disease spreads is dependent upon interactions between environmental factors, the reproductive and dispersive nature of the pathogen and the nature of host resistance. Providing environmental and pathogen factors are uniform, differences in disease gradients among cultivars may be used to help characterise levels of QR. However, disease gradients alone are not considered to be reliable indicators of partial resistance (Berger and Luke, 1979; Luke and Berger, 1982; Headrick and Pataky, 1988), and should be interpreted in conjunction with infection rates (MacKenzie, 1976; Minogue, 1986).

The development of a mathematical model that satisfactorily describes disease increase in both space and time (spatiotemporal) has long been a goal of epidemiologists. In attempting to combine disease gradients with levels of infection,

Berger and Luke (1979) introduced the concept of isopathic rates, which are a measure of the rate of movement of isopaths (annuli of disease of equal intensity). Isopathic rates are therefore a measure of the velocity of spread and are expressed in units of distance per time, for example, metres per day. Berger and Luke (1979) calculated the velocity of spread of crown rust in three oat cultivars by dividing the distance between plants at two points along a disease gradient, A and B, by the time taken for disease at point B to reach the level of disease observed at point A. They used isopathic rates to rank cultivar resistance. In a similar way, Alderman, Nutter and Labrinos (1989) used the model proposed by Minogue and Fry (1983) to analyse the spatial and temporal aspects of spread of late leaf spot (*Cercosporidium personatum* [Berk.&Curt.] Deighton) of peanut (*Arachis hypogaea* L.). They calculated the velocity (v) of a disease isopath from a source as $v = r/b$, where r is the apparent infection rate defined by van der Plank (1963) and b is the slope of the disease gradient.

Other generalised models, that attempt to describe spatiotemporal aspects of disease increase have been developed. These include the focus-expansion model of van den Bosch *et al.* (1988) and van den Bosch, Zadoks and Metz (1988) and the use of spatiotemporal statistics (Cliff and Ord, 1981; Reynolds and Madden, 1988). These models generally allow for more complex estimation of epidemic parameters such as disease gradients and velocities of spread. However, details of disease progress are often lost through the use of assumptions, linearisation and mathematical estimation. A problem that has precluded the development of satisfactory spatiotemporal models has been the difficulty in finding a transformed dependent variable that fits both disease progress and spread and therefore adequately describes the entire epidemic (Headrick and Pataky, 1988).

Three-dimensional surface plots of disease progress in time and space can reveal details that are not easily visualised when disease progress is modeled in time and space separately. Using untransformed data, Headrick and Pataky (1988) plotted three-dimensional response surfaces of common rust (*Puccinia sorghi* Schwein.) epidemics in susceptible and partially resistant sweet corn hybrids. They found that

the response curves discerned particular "characteristics" in some hybrids that were hidden by transformation models. The disadvantage of using untransformed (non-linear) data is that linear regression coefficients of disease gradients and progress cannot be used to compare epidemics. One is therefore faced with the dilemma of using an empirical model that permits biological interpretations but not comparisons, or a mathematical model that allows epidemics to be compared, but may hide some of the underlying biological detail. Headrick and Pataky (1988) proposed that infection rates be used in conjunction with response surfaces and/or isopathic rates when comparing partial resistance of corn cultivars to common rust. Alderman, Nutter and Labrinos (1989) also used three-dimensional surface plots to describe spatial and temporal spread of late leaf spot in peanut.

The disease ratings given to the selections described in Chapter 4 were uncertain and could not be relied upon with confidence, because they were derived from a single non-replicated field experiment. The effects of interference, environment and other factors associated with evaluating resistance in the field have been discussed previously. The development of a field screening method with which the greenhouse screening assay could be correlated, was considered to be a pre-requisite to the development of an integrated procedure for screening sunflower for resistance to *A. helianthi.* Ideally, a reliable method of field screening should be available prior to the development of a greenhouse assay. However, by nature, field screening is slow and hence, could not precede the development of the greenhouse assay, but instead, would need to be developed over years and locations.

Previously, the assessment of resistance was performed at a critical point - flowering to post flowering (Allen, 1981) - when the inoculum load was high and predisposition to susceptability due to plant age was increasing. A major problem of using the critical point model is that disease assessment occurs at or after flowering. This means that for the purposes of selection and inbreeding, large numbers of plants would have to be bagged prior to flowering to prevent outcrossing. In a large selection trial containing many thousands of plants, this clearly represents a logistical

problem. If some measure of resistance could be obtained prior to flowering, then only selected plants would need to be bagged, thus saving much time and labour.

The field experiments described in this chapter were conducted to establish an accurate and reliable method of selecting sunflower lines with resistance to *A. helianthi*. Isolated, multiple-row plots of each sunflower line were replicated at two locations. Several epidemic parameters were determined for each sunflower line tested in order to generate a range of descriptive variables that could be tested for correlations with resistance parameters measured in the greenhouse (Chapter 7). Various statistical methods were applied to determine which epidemic parameters, disease severity rating (critical point), audpc, apparent infection rate, velocity of spread or disease gradient would be most useful for differentiating lines with quantitative resistance. Three-dimensional surface plots were also generated for each sunflower line to give an overall picture of disease progress in space and time. Volumes beneath the surface plots were calculated to give a parameter representing disease spread in space and time.

Ten sunflower lines were selected for this study, based on their reactions to *A. helianthi* obtained from the initial selection trial (Chapter4). Lines were selected to represent a range of reactions from resistant to susceptible.

5.3 Materials and Methods

5.3.1 Field trial sites and trial design

Sites at two Queensland Department of Primary Industries field research stations were selected for the trials. These were located in the Lockyer Valley, east of Toowoomba and at Kingsthorpe on the Darling Downs west of Toowoomba (see Figure 1.1, Chapter 1). These will be referred to hereafter as Site 1 and Site 2 respectively. Since Site 1 was at an elevation of about 100m above sea level and Site 2 was at 600m above sea level, climate was expected to differ between the two sites. Slightly cooler growing conditions at Site 2 were expected to delay both plant maturity and epidemic development and result in a different epidemic pattern than that at Site 1.

Pre-planting cultivation was performed at both sites to remove weeds and prepare a good seedbed for plant establishment.

A randomised complete block design with three replicates was used to evaluate 10 lines (Table 5.1). These comprised a subset of the lines described in Table 4.3 (Chapter 4) and represented a range of reaction types. Each replicate consisted of 10 individual plots arranged as two blocks of 5 plots. Each plot was $25m^2$ (5x5m) and consisted of 7 rows, 0.8m apart and 4.8 m long. Plants were spaced at 0.2m. An interplot space of 4.2m was used to separate plots. The susceptible line B89 was sown in the centre row of every plot on the 20th November, 1994. At the same time, the 4.2 m interplot space was sown with 2 rows of forage sorghum, variety "Cow Chow" (Pioneer Hi-Bred Australia Pty Ltd). This was intended to act as a buffer between plots to reduce interplot interference. Irrigation was applied to assist seed germination. The remaining 6 rows of each plot were planted on the 5th December 1994 with seed of one of the lines being tested.

These specifications were repeated at Site 2 one day later than at Site 1.

Rainfall and temperature data were collected at both sites from the time of inoculation of spreader rows until the last assessment date.

Table 5.1. *Experiment codes, pedigrees, selection codes and reactions to A. helianthi of 10 sunflower lines selected for field evaluation.*

Pedigree Code	Pedigree	Single plant selections	[a]Reaction type
P_1	ARpop//Rpop/Charata	10020-11-1-18	1
P_8	ARpop//QSR1	10014-6-1-11	2
P_9	ARpop//QSR1	10008-3-3-5	1
P_{10}	Arpop//Rx677	10007.13.2.7	2
P_{13}	HA-B89	—	4
P_{14}	[b]Hysun 45 CQ	—	?
P_{15}	QSR1	—	2
P_{16}	Charata-3-2-1	—	3
P_{17}	RX677	—	3
P_{18}	Rpop	—	4

[a] *Reaction types 1, 2, 3 and 4 = 0-5%, 6-10.9%, 11-15.9% and >16% of leaf area infected on the lowest pair of unsenesced leaves respectively.*

[b] *Commercial hybrid of Pacific Seeds Australia Pty Ltd.*

? = *Reaction type unknown, but the line was marketed as being resistant to* A. helianthi.

5.3.2 Inoculation of plants and assessment of disease

Plants of B89 in the centre "spreader" row of each plot were spray inoculated with conidia of *A. helianthi* using a 5L garden sprayer. Inoculum was produced on sunflower leaf extract agar (SLEA) as described by Kong, Kochman and Brown, (1995). Plants (V6-V8 growth stage) at both sites were inoculated on the 20th December 1996 then again 10 and 20 days later. Following each inoculation, overhead misting was applied to all plots for 6-8 h per day, on 4 consecutive days. Thereafter, misting was applied for a 4-6 h period on alternate days, depending on rainfall, until plants were at the budding stage.

Plots were examined weekly to assess the development of disease on plants adjacent to the spreader rows in each plot. Rating of disease severity commenced at Site 1 on the 25th January 1995 (50 days after planting) when the majority of lines were at the R0-R2 growth stage. Epidemic development at Site 2 was much slower and rating did not commence until 5th January 1995 (62 days after planting) when plants were at the R4-R5 growth stage. The stems of plants were marked with red paint at positions corresponding to the location of the 3rd pair of leaves and also at points corresponding to the middle of the plant height and just below the position of the flower bud. These positions will be referred to as the 'low', 'middle' and 'upper' leaf positions respectively. Percentage leaf area infected was recorded on leaves at these positions using a modification of the pictorial key developed by Allen, Brown and Kochman, (1983c). The modified key has more severity classes in the range of 0-15% leaf area infected than the original key. An average value for each leaf pair was recorded and subsequently used for data analyses. This value will be referred to as the disease severity rating or DSR for each line.

Three plants in each row were assessed as described. These included a plant in the middle of the row and the 3rd plant from each end of the row. Plants at Site 1 were rated at 50, 56, 65, 72 and 78 days after planting. Plants at Site 2 were rated at 62, 72,

78 and 84 days after planting. Plants at the last rating date at both sites were at the R8-R9 growth stage. The same leaves in the low, middle and upper positions were assessed at each rating time. Data for percentage leaf area infected was obtained for all lines except for P10, which developed a physiological disorder that caused necrotic spots to develop on leaves. These spots were almost indistinguishable from the lesions caused by *A. helianthi* (see Figure 2.1, Chapter 2)

5.3.3 Data Analysis

The analytical strategy applied to the data collected from the field experiments was to 1) generate parameters for each sunflower line that described epidemic development in space and time; 2) apply a means separation statistic, Sheffe's Significant Difference (SSD), to reveal the extent to which each parameter separated the sunflower lines; 3) test the correlation between parameters using Spearman's rank correlation, to identify parameters that could be used to select sunflower lines with resistance to *A. helianthi*.

The computer program Systat 5.02 for Windows (Wilkinson and Vang, 1992) was used for analysis of variance (AOV), for pairwise comparisons of treatment means and for linear regression and Spearman's rank correlation. The computer program Microsoft Excel 5.0 for Windows (Microsoft Corporation, 1995) was used to transform data, to generate linear regression statistics and to calculate audpcs. The computer program Surfer 5.0 for Windows (Golden Software Inc., 1994) was used to generate three-dimensional surface plots of disease progress in space and time.

A disease severity rating (DSR) was calculated for each plant by averaging the percentage leaf area infected for the leaf pairs in the lower, middle and upper positions. All other epidemic parameters were determined from the DSRs for each plant. Plots of disease progress indicated that the epidemics for each line developed as two distinct phases - an 'early' phase and a 'late' phase. Audpc's, apparent infection rates and velocities of spread were calculated for each phase and for the complete epidemic. Audpc's were calculated using the trapezoidal rule as described previously and apparent infection rates were determined as the slope of the line

obtained from the regressions of percentage leaf area infected with time after planting. Data were transformed using the logit and gompit transformation models prior to regression analysis. Disease severity for each plant was determined as the average disease rating (percentage leaf area showing disease symptoms) of leaves in the low, middle and upper positions as described previously. Disease severity, audpc's, apparent infection rates and velocities of spread were calculated for every plant that was rated. That is, 21 plants per plot x 3 replicates, for each site. The means for the audpc's, apparent infection rates and velocities of spread for each line were compared using SSD test. Epidemic parameters for the spreader row in each plot were used as covariates in each analysis.

Disease gradients (b) were calculated by regressing log-transformed percentage leaf area infected with linear distance (m) from the line source of infection (spreader row). Gradients were determined for each rated-plant position in each plot and for each assessment date. That is, for the 3 plants in each row and for the rows on either side of the spreader row, giving a total of 6 gradients per plot. Gradients for each phase of the epidemic were calculated as the average of gradients for assessment dates within a particular phase. For example, the average of gradients determined at 50, 56 and 65 days after planting at Site 1 were averaged to find the gradient for the "early' phase of the epidemic. The average of gradients for all assessment dates was taken as the gradient for the complete epidemic. SSD test was used to compare gradients of sunflower lines at each phase of the epidemic.

The velocity of spread (v) of disease was calculated for each line by dividing the apparent infection rate for each phase of the epidemic (r) by the average disease gradient (b) for each phase. Velocities of spread for each sunflower line were compared using SSD test.

Actual (untransformed) data for the percentage leaf area infected was used to generate surface response maps of disease progress in space and time. Percentage leaf area infected was taken as the mean of ratings determined for the low, middle and upper positions on rated plants of each sunflower line. "Kriging" rather than the commonly

used "inverse distance" gridding method was chosen to estimate grid references. Kriging is a flexible geostatistical gridding method that incorporates a linear variogram model to interpolate each grid node. Maps were generated using a contour inteval equal to 2.0 % leaf area infected. Grid volumes (GVs), or the volume beneath the surface plot of disease progress in space and time for each sunflower line, were calculated using the trapezoidal rule. SSD test was used to compare the GVs of each line.

Spearman's rank correlation was used to determine the relationship between the disease severity at each rating time, the audpc, the apparent infection rate, the disease gradient, the velocity of spread and the grid volume. Parameters with correlation coefficients of ≥ 0.7 were considered to be well correlated. Each epidemic parameter was evaluated according to it's ability to separate the sunflower lines and their degree of correlation with disease severity ratings (DSR). Patterns and characteristics revealed by these spatial and temporal epidemic parameters were used to draw inferences about epidemic development in each sunflower line.

The DSRs for the low plant position were regressed with the DSRs for the middle and upper plant positions, for all lines grown at field Site 1 and for all rating times. Coefficients of determination were used to determine the extent to which disease levels at any particular plant position predicted disease levels at other plant positions.

5.4 Results

5.4.1 Rainfall and temperature data

Daily rainfall and average daily temperatures for Sites 1 and 2 are shown in Figures 5.1 and 5.2 respectively. Average daily temperatures at both sites ranged from 20-25°C throughout most of the rating period. However, higher temperatures, ranging from 25-30°C, were experienced at Site 2 from 81-84 days after planting. Overcast, wet conditions persisted from 68-76 days after planting at Site 1 and despite overcast conditions for a similar period at Site 2, no rainfall was recorded. A small amount of

rain fell at Site 2, at the beginning and at the end of the rating period. The extended period of wet weather at Site 1, together with warm conditions, was highly conducive to epidemic development. Drier conditions at Site 2 were less favourable to epidemic development.

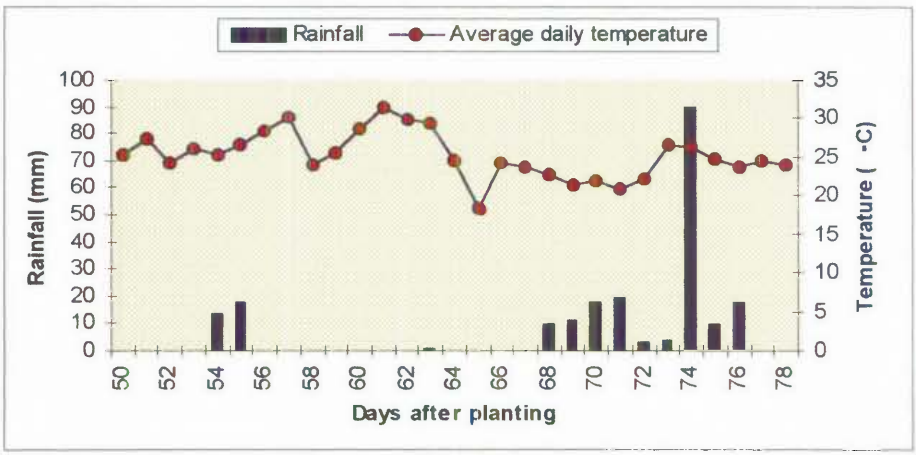

Figure 5.1. *Average daily temperatures and rainfall recorded at Site 1 from 50 (first disease assessment) to 78 (last disease assessment) days after planting.*

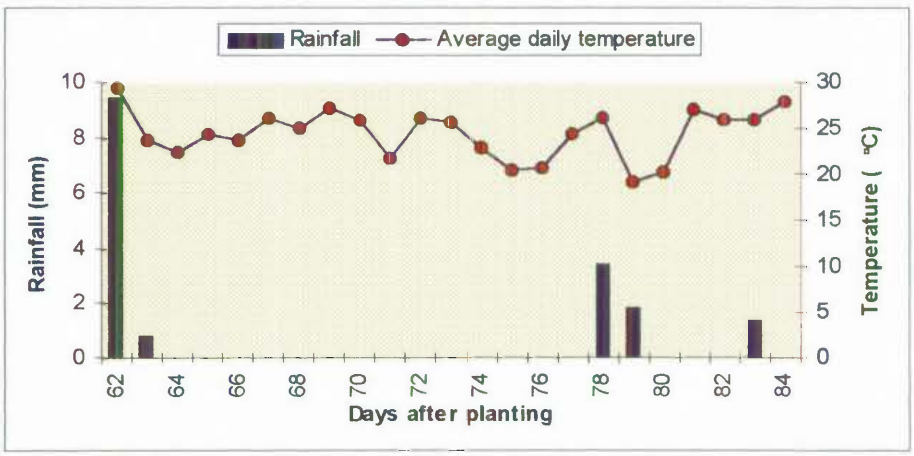

Figure 5.2. *Average daily temperatures and rainfall recorded at Site 2 from 62 (first disease assessment) to 84 (last disease assessment) days after planting.*

5.4.2 Plant phenologies throughout the rating period

Because the lines at the two sites were not always rated at the same number of days after planting, it was difficult to make direct comparisons of maturity between sunflower lines at the two sites. Lines were however, rated at 72 and 78 days after planting at both sites and could be compared at these times. In general, the lines at Site 1 were at a more advanced stage of maturity on these days, than those at Site 2 (Table 5.2). At both sites, line P9 had a much slower maturity than all other lines, whereas lines P17 and P18 matured faster than all other lines. The remaining lines matured at a similar rate, although there were some minor differences between sites for some lines.

Table 5.2. *Growth stages of sunflower lines at Sites 1 and 2 recorded at their respective rating times.*

	Site1					Site2			
Sunflower	Days after planting								
line	50	56	65	72	78	62	72	78	84
P_1	[a]1	4	5.5	6	7	1	5.1	5.9	7
P_8	0	3	5.2	5.6	8	5.0	5.5	6	8
P_9	0	2	4	5.2	5.4	3	4	5.3	5.6
P_{13}	2	4	5.7	7	8	3	5.7	6	7
P_{14}	2	4	5.9	6	8	4	5.5	7	7
P_{15}	0	2	5.0	5.9	6	4	5.2	5.9	7
P_{16}	1	4	5.2	5.9	6	4	5.2	5.9	7
P_{17}	3	5.1	5.9	7	8	5.1	6	7	8
P_{18}	3	5.9	6	7	8	5.6	7	7	8

[a] *All growth stage increments are for the reproductive (R-) phase of growth.*

5.4.3 Disease progress in time

(i) Disease Severity

Table 5.3 shows the mean percentage leaf area infected per plant for each sunflower line grown at Sites 1and 2. The differences between the means of each sunflower line indicated by SSD test, varied with site and time.

Table 5.3. *Disease severity ratings (DSRs) for each rating time, determined as the mean percentage leaf area infected per plant, of lines grown at Sites 1 and 2. Values with the same letter are not significantly different.*

	Site 1					Site 2			
Sunflower	Days after planting					Days after planting			
Line	50	56	65	72	78	62	72	78	84
P1	0.05 d	0.17 d	0.48 de	2.30 c	37.10 f	0.43 d	0.18 c	0.85 e	12.58d
P8	0.09 c	0.55 b	1.25 b	6.58 b	51.68 d	0.22 b	0.53 b	4.73 b	27.18 b
P9	0.05 d	0.23 c	0.45 e	2.09 c	24.44 g	0.13 cd	0.26 c	2.24 d	9.76 d
P13	0.09 c	0.92 a	2.22 a	17.7 a	72.29 a	0.36 a	1.89 a	8.04 a	29.9 b
P14	0.06 cd	0.31 c	0.51 de	3.25 c	42.81 e	0.13 c	0.25 c	1.94 d	19.44 c
P15	0.21 a	0.82 a	0.81 cd	5.9 b	46.19 d	0.13 c	0.33 c	3.10 cd	20.02 c
P16	0.13 bc	0.60 b	1.09 bc	7.14 b	57.51 c	0.14 c	0.30 c	3.69 c	29.46 b
P17	0.05 d	0.32 c	0.66 d	2.76 c	35.61 f	0.12 c	0.27 c	2.19 d	16.00 c
P18	0.15 b	0.29 c	0.98 c	6.89 b	80.03 b	0.16 bc	0.42 bc	2.60 d	37.79 a

At Site 1, the nine sunflower lines were separated into 4 or 5 groups at 50, 56, 65 and 72 days after planting, and into 7 groups at 78 days after planting, when disease intensity was greatest. Lines P_1, P_9, P_{14} and P_{17} were the most resistant and lines $P_{13}$and P_{18} the most susceptible. Lines P_8, P_{15} an P_{16} had moderate resistance. At Site 2, the nine sunflower lines were separated into 4 or 5 groups at 62, 72, 78 and 84 days after planting. Lines P_1 and P_9 were the most resistant and lines P_8, P_{13} and P_{18} the most susceptible to *A. helianthi.*

Spearman's correlation coefficients for the rankings of lines at each site give an indication of the relative performance of the lines under different environmental conditions and disease intensities (Table 5.4).

Table 5.4: *Spearmans's correlation coefficients for rankings of sunflower lines at Sites 1 and 2 for each assessment time. Rankings were based on disease severity ratings (DSRs) determined as the mean percentage leaf area infected per plant. Rankings at these two sites were also compared with the ranking obtained for the same lines in the non-replicated field screening experiment conducted in 1991.*

	[a]$Site1_{50}$	$Site1_{56}$	$Site1_{65}$	$Site1_{72}$	$Site1_{78}$	Field 91
[a]$Site2_{62}$	0.56	0.58	0.85	0.83	0.80	0.65
$Site2_{72}$	0.64	0.72	0.90	0.80	0.75	0.69
$Site2_{78}$	0.60	0.80	0.88	0.80	0.67	0.57
$Site2_{84}$	0.78	0.57	0.87	0.95	0.98	0.86
Field 91	0.50	0.64	0.69	0.86	0.76	1.00

[a] *Subscripts refer to the number of days after planting.*

The correlation between the two sites was poor (0.56) at the first assessment time, moderate (0.72) at the second assessment time and high (0.88, 0.95) at the third and fourth assessment times. The ranking of lines at the last assessment time for each site was highly (0.98) correlated. In general, the correlations between sites and rating times were moderate to high.

Coefficients for the correlation between rankings at Sites 1 and 2 and rankings obtained for the same sunflower lines in the non-replicated field trial conducted in 1991 (Chapter 4), are also given in Table 5.4. The rank order of lines at Site 1, at 72 and 78 days after planting, was highly correlated (0.86 and 0.76 respectively) with the rank order obtained in 1991 (based on disease severity data Chapter 4, Table 4.2). The rank order of lines at Site 2, at 84 days after planting, was highly correlated (0.86) with the rank order obtained in 1991.

(ii) Disease progress curves

Figure 5.3 shows the progress of disease development with time for each sunflower line at Sites 1 and 2. The mean percentage leaf area infected per plant was used to plot disease progress for each sunflower line. The resulting line graphs show disease progress for each sunflower line, its corresponding spreader row and the susceptible line, B89 (P_{13}). For all lines and at both sites, disease progress was characterised by two distinct phases. At Site 1, disease progress from 50 to 65 days after planting was taken to represent the 'early' phase of the epidemic, while disease progress from 65 to 78 days after planting was taken to represent the 'late'phase. At Site 2, these phases were delineated as 62 to 72 and 72 to 84 days after planting respectively (Figure 5.3). At Site 1, the increase in disease intensity coincided with overcast weather and light rainfall beginning at 68 and ending at 78 days after planting (Figure 5.1). Similarly at Site 2, overcast weather and light rainfall at 78 and 79 days after planting resulted in an increase in disease intensity (Figure 5.2). During these wet periods, the sunflower lines at both sites were at mid- to late flowering (Table 5.2).

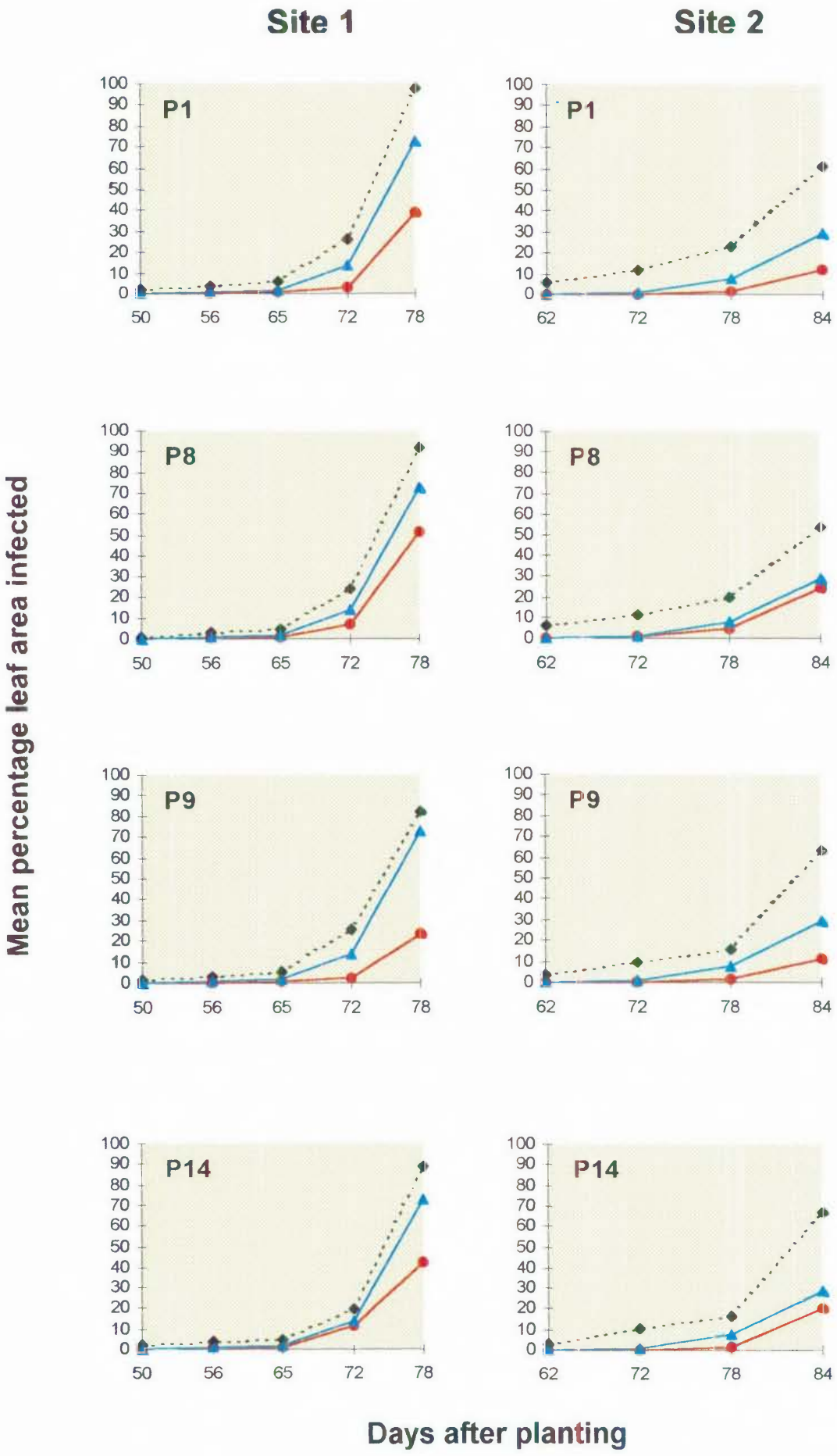
Site 1
Site 2
P1
P8
P9
P14
Mean percentage leaf area infected
Days after planting
0
10
20
30
40
50
60
70
80
90
100
50
56
65
72
78
62
84

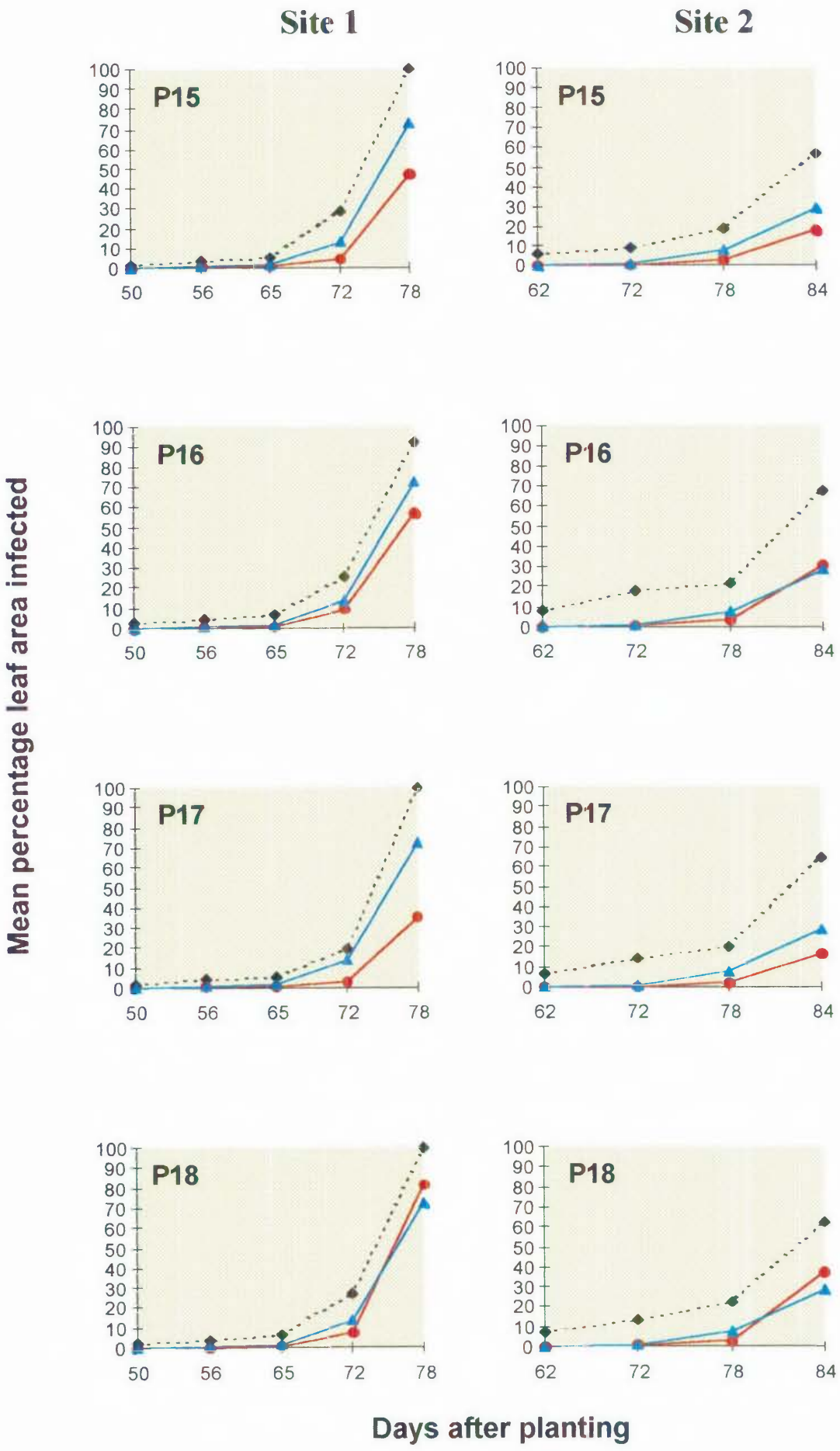
Site 1
Site 2
P15
P16
P17
P18
Mean percentage leaf area infected
Days after planting
0
10
20
30
40
50
60
70
80
90
100
50
56
65
72
78
62
84

Figure 5.3. *Disease progress curves for sunflower lines evaluated at Gatton (Site1) and Kingsthorpe (Site 2) field research stations. Plots are of mean percentage leaf area infected for plants in the spreader row in each plot* (···◆···), *the susceptible line, B89* (—▲—) and the tested lines (—●—).

Disease intensity at Site 1 was considerably higher than that experienced at Site 2. By 78 days after planting, the average percentage leaf area infected was 90-100% for plants in the spreader rows at Site 1, and ranged from 60-70% at Site 2. The proportion of diseased tissue for lines grown at Site 1 was accordingly greater than the proportion of diseased tissue of lines grown at Site 2. For example, at 78 days after planting, the mean percentage of leaf area infected per plant ranged from 24.44 80.03 for lines at Site 1 (Table5.3). This can be compared with 9.76 37.79 % at Site 2 (Table5.3), 84 days after planting when lines were at an equivalent growth stage to those at Site 1 (Table 5.2).

(iii) Apparent infection rate

Table 5.5 shows the apparent infection rates (r) for the 9 sunflower lines tested at the two field sites. These were calculated by regressing untransformed, log- and gompertz- transformed data (logit y and gompit y) for percentage leaf area infected, with time. The coefficients of determination (R^2) for the regressions give an indication of the extent of linear co-relation between percentage leaf area infected and time. The R^2 values are therefore taken to indicate the goodness-of-fit of the regression equations applied to the data. Apparent infection rates calculated from untransformed data generally had low coefficients of determination, indicating a poor fit of the data to the regression and hence poor estimates of apparent infection rate, r. At Site 1, the regression of log-transformed data gave a better fit than did the gompertz-transformed data. At Site 2, the regression of log-transformed data gave a marginally better fit than did the gompertz-transformed data. Sunflower lines were therefore compared using apparent infection rates calculated from log-transformed data for percentage leaf area infected.

Table 5.6 shows the apparent infection rates (r) of the 9 sunflower lines for the 'early'(r_e), 'late' (r_l) epidemic phases and for the 'complete' (r_c) epidemic. At Site 1,

the 9 lines were clustered into either 3 or 4 discrete groups. Line P_9 had the highest and lowest rates of infection for the 'early' and 'late' epidemic phases respectively. However, the averaging affect arising from the calculation of r_c caused P_9 to have a moderately high apparent infection rate overall. During the 'early' phase of the epidemic, P_1, P_{14}, P_{15}, P_{16} and P_{18} had the lowest rates of infection. Line P_{18} had the highest rate of infection during the 'late' epidemic phase and overall, it had the highest apparent infection rate together with line P_{13}. Line P_{15} had the lowest infection rate overall.

Table 5.5. *Apparent infection rates (r) of 9 sunflower lines and their coefficients of determination (R^2) calculated from the regressions with time of untransformed, log- and gompertz- transformed data for percentage leaf area infected.*

Field Site	Sunflower line	Untransformed		Logistic model		Gompertz model	
		[a]Rate (*r*)	R^2	Rate (*r*)	R^2	Rate (*r*)	R^2
1	P1	1.03	0.50	0.12	0.87	0.03	0.73
2		0.47	0.59	0.14	0.94	0.03	0.84
1	P8	1.43	0.36	0.11	0.94	0.03	0.80
2		0.98	0.64	0.13	0.87	0.03	0.83
1	P9	0.63	0.53	0.10	0.92	0.02	0.83
2		0.41	0.62	0.13	0.88	0.02	0.86
1	P13	2.19	0.65	0.12	0.95	0.05	0.82
2		1.23	0.70	0.11	0.91	0.03	0.88
1	P14	1.15	0.51	0.10	0.88	0.03	0.73
2		0.80	0.55	0.15	0.82	0.04	0.75
1	P15	1.32	0.55	0.09	0.87	0.03	0.75
2		0.73	0.62	0.12	0.71	0.03	0.79
1	P16	1.61	0.55	0.10	0.90	0.03	0.76
2		1.22	0.60	0.12	0.86	0.03	0.79
1	P17	0.99	0.51	0.11	0.89	0.03	0.76
2		0.65	0.60	0.11	0.91	0.03	0.86
1	P18	2.25	0.52	0.12	0.87	0.05	0.68
2		1.46	0.56	0.13	0.78	0.04	0.77

[a] *Apparent infection rate in units per day.*

Table 5.6. *Apparent infection rates (r) for 9 sunflower lines grown at two field sites. Values with the same letter are not significantly different.*

Sunflower line	Site 1			Site 2		
	Apparent infection rate					
	$^{a}r_e$	$^{b}r_l$	$^{c}r_c$	r_e	r_l	r_c
P_1	0.07 c	0.16 c	0.10 c	0.13 a	0.18 b	0.14 a
P_8	0.10 b	0.16 c	0.12 b	0.11 bc	0.19 b	0.13 ab
P_9	0.13 a	0.12 d	0.12 b	0.13 a	0.15 c	0.13 ab
P_{13}	0.10 b	0.19 b	0.13 a	0.10 c	0.14 d	0.10 c
P_{14}	0.07 c	0.17 c	0.10 c	0.12 ab	0.22 a	0.15 a
P_{15}	0.05 c	0.16 c	0.09 d	0.11 bc	0.20 ab	0.12 b
P_{16}	0.06 c	0.17 c	0.10 c	0.09 c	0.19 b	0.12 b
P_{17}	0.10 b	0.16 c	0.12 b	0.10 c	0.15 c	0.11 bc
P_{18}	0.07 c	0.24 a	0.13 a	0.10 c	0.19 b	0.13 ab

$^{a}r_e$ = Represents apparent infection rate in units d^{-1} for the 'early' phase of the epidemic.
$^{b}r_l$ = Represents apparent infection rate in units d^{-1} for the 'late' phase of the epidemic.
$^{c}r_c$ = Represents apparent infection rate in units d^{-1} for the 'complete' epidemic.

At Site 2, the 9 sunflower lines were clustered into 4 or 5 groups for each phase of the epidemic, but some of these groups were overlapping. During the 'early' epidemic phase, lines P_1 and P_9 had the highest infection rates and lines P_{13}, P_{16}, P_{17} and P_{18} had the lowest infection rates. During the 'late'epidemic phase, line P_{14} had the highest and line P_{13} the lowest, infection rates. Overall, lines P_1 and P_{14} had the highest infection rates and P_{13} had the lowest infection rates.

(iv) Area under the disease progress curve (audpc)

At Site 1, the 9 sunflower lines were separated into 5 or 6, mostly discrete, groups on the basis of audpc (Table 5.7). However at Site 2, although up to 9 groups were identified, several groups were overlapping. At both sites, line P_{13} had the largest audpc for all epidemic phases, while overall, lines P_1, P_9 and P_{17} had the smallest audpc's.

Table 5.7. *Area under the disease progress curve (audpc) for 9 sunflower lines grown at two field sites. Values with the same letter are not significantly different.*

Sunflower line	Site 1			Site 2		
	[a]$audpc_e$	[b]$audpc_l$	[c]$audpc_c$	$audpc_e$	$audpc_l$	$audpc_c$
P_1	3.3 d	128.1 e	129.3 e	6.4 d	44.5 f	46.6 f
P_8	10.2 b	204.3 c	216.9 c	23.2 b	126.1 bc	130.3 bc
P_9	4.1 d	90.9 f	95.9 f	11.7 cd	56.8 ef	63.4 ef
P_{13}	17.1 a	332.6 a	348.2 a	42.8 a	169.7 a	181.1 a
P_{14}	4.8 d	157.0 d	162.4 d	10.8 cd	82.3 de	89.1 d
P_{15}	10.4 b	176.8 d	186.9 d	15.5 c	92.7 d	95.7 cd
P_{16}	9.7 b	222.4 c	230.4 c	15.8 c	117.3 c	114.1 c
P_{17}	5.7 cd	129.6 e	137.7 e	11.3 cd	67.4 e	68.4 e
P_{18}	7.0 c	286.2 b	292.3 b	15.1 c	136.7b	138.6 b

[a]$audpc_e$ =Represents the area under the disease progress curve for the 'early' phase of the epidemic.

[b]$audpc_l$ = Represents the area under the disease progress curve for the 'late' phase of the epidemic.

[c]$audpc_c$ = Represents the area under the disease progress curve for the complete epidemic.

5.4.4 Disease progress in space

(i) Disease gradients

Table 5.8 shows the disease gradients (*b*) of the 9 sunflower lines tested at the two field sites. In general, the lines were not well separated at either site and tended to be clustered into 3 to 5 groups, some of which were overlapping. For example, at Site 1 during the 'early' phase of the epidemic, 6 of the 9 lines had the same values for *b*. This clustering of lines in overlapping groups limited the differentiation of the lines, except for extreme values of *b*. Thus, at Site 1, lines P_9 and P_8 had the steepest disease gradients throughout the epidemic and overall, line P_{14} had the flattest disease gradients for all phases of the epidemic. However, lines P_{15}, P_{16} and P_{18} also had relatively flat gradients during the 'late' phase of the epidemic.

At Site 2, the general pattern showed that P_1 and P_9 had the steepest and P_{18} the flattest disease gradients for all phases of the epidemic. Lines P_{15}, P_{16} and P_{17} also had relatively flat disease gradients during the 'early' phase of the epidemic and the susceptible line P_{13} had steep disease gradients.

Table 5.8. *Disease gradients (b) of 9 sunflower lines grown at Site1 and Site 2. Values with the same letter are not significantly different.*

Sunflower Line	Site 1			Site 2		
	b_e	b_l	b_c	b_e	b_l	b_c
P_1	0.25 bc	0.12 bc	0.19 cd	0.78 a	0.52 ab	0.72 a
P_8	0.32 bc	0.30 a	0.34 b	0.62 ab	0.50 ab	0.56 ab
P_9	0.57 a	0.28 ab	0.46 a	0.75 a	0.54 a	0.70 a
P_{13}	0.26 bc	0.20 b	0.24 c	0.62 a	0.39 b	0.51 b
P_{14}	0.21 c	0.06 c	0.14 d	0.60 ab	0.33 b	0.48 b
P_{15}	0.35 b	0.11 c	0.24 c	0.50 b	0.45 ab	0.47 b
P_{16}	0.29 bc	0.11 c	0.22 cd	0.49 b	0.38 b	0.43 bc
P_{17}	0.27 bc	0.16 bc	0.20 cd	0.50 b	0.39 b	0.47 b
P_{18}	0.26 bc	0.06 c	0.17 cd	0.36 b	0.16 c	0.28 c

b_e = Represents the average of gradients measured at 62, 72 and 78 days after planting.
b_l = Represents the average of gradients measured at 72, 78 and 84 days after planting.
b_c = Represents the average of gradients measured at 62, 72, 78 and 84 days after planting.

5.4.5 Disease progress in space and time

(i) Surface response maps

Figure 5.4 shows the three dimensional plots of *A. helianthi* epidemics in all sunflower lines at both field sites. Untransformed disease severity data (z axis) was plotted against time (x axis) and distance (y axis) from the infection focus. Contour lines represent isopaths connecting points of equal disease severity. The maps clearly show isopath movement in both space and time. The interrelationships of disease spread in both space and time are made visible on these maps. Isopathic rates can be discerned as the temporal difference in the course of any given isopath with distance. Overall, isopathic rates were faster at Site1 than at Site 2. Line P_9 had the slowest isopathic rate and the steepest disease gradient at the last rating time. Disease gradients were generally steeper at Site 2 where disease intensity was lower. Gradients were related to isopathic rates, such that isopathic rates decreased with increases in gradient. The rate of disease progress was indicated by the distance between isopaths. The small distances between isopaths in lines P_8, P_{13}, P_{16} and P_{18} indicate fast rates of disease increase, while the wide spaces between isopaths in P_9 indicate a relatively slow rate of disease increase. Rates of disease increase were much slower at Site 2.

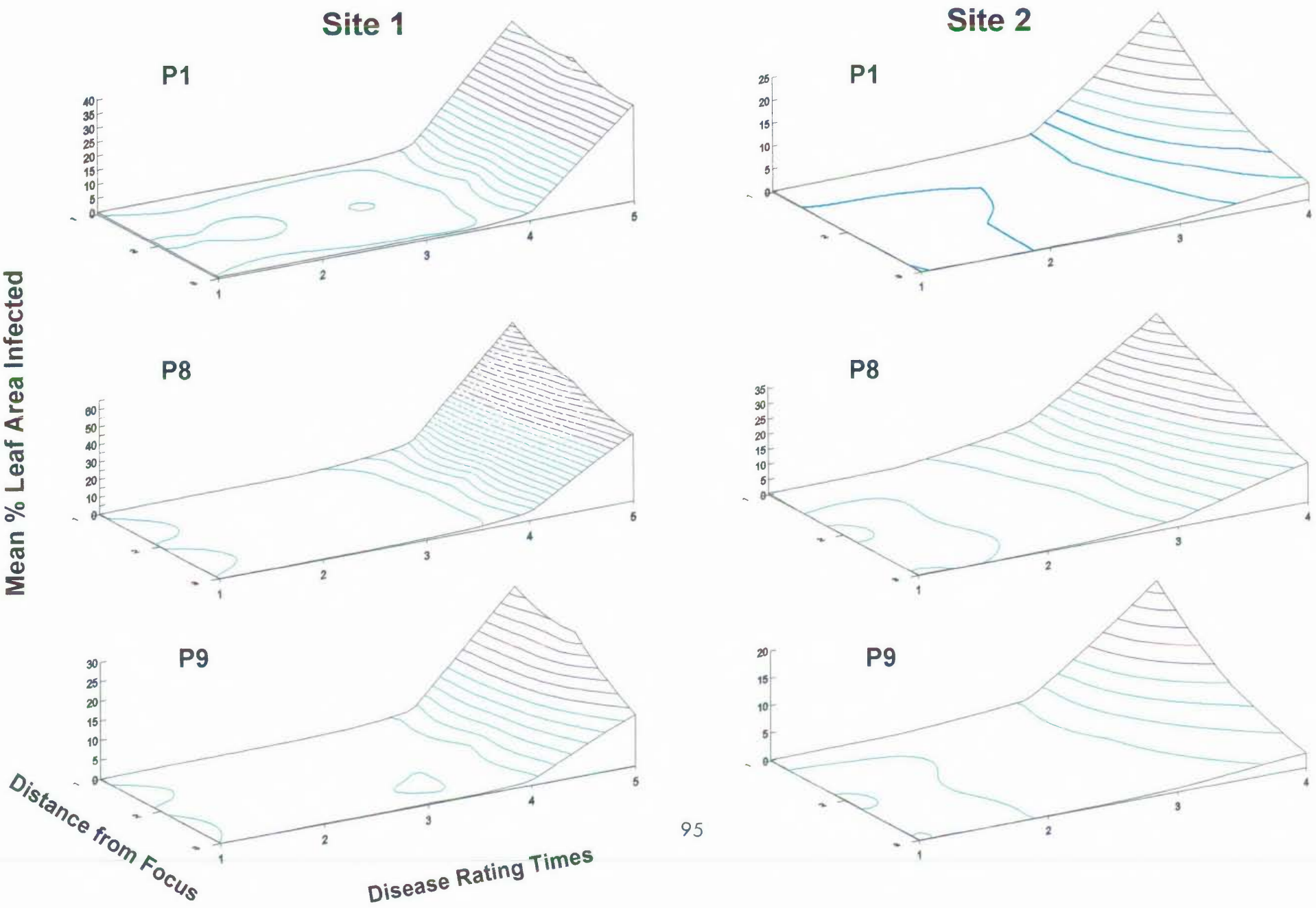
Site 1
P1
P8
P9
Site 2
P1
P8
P9
Mean % Leaf Area Infected
Distance from Focus
Disease Rating Times

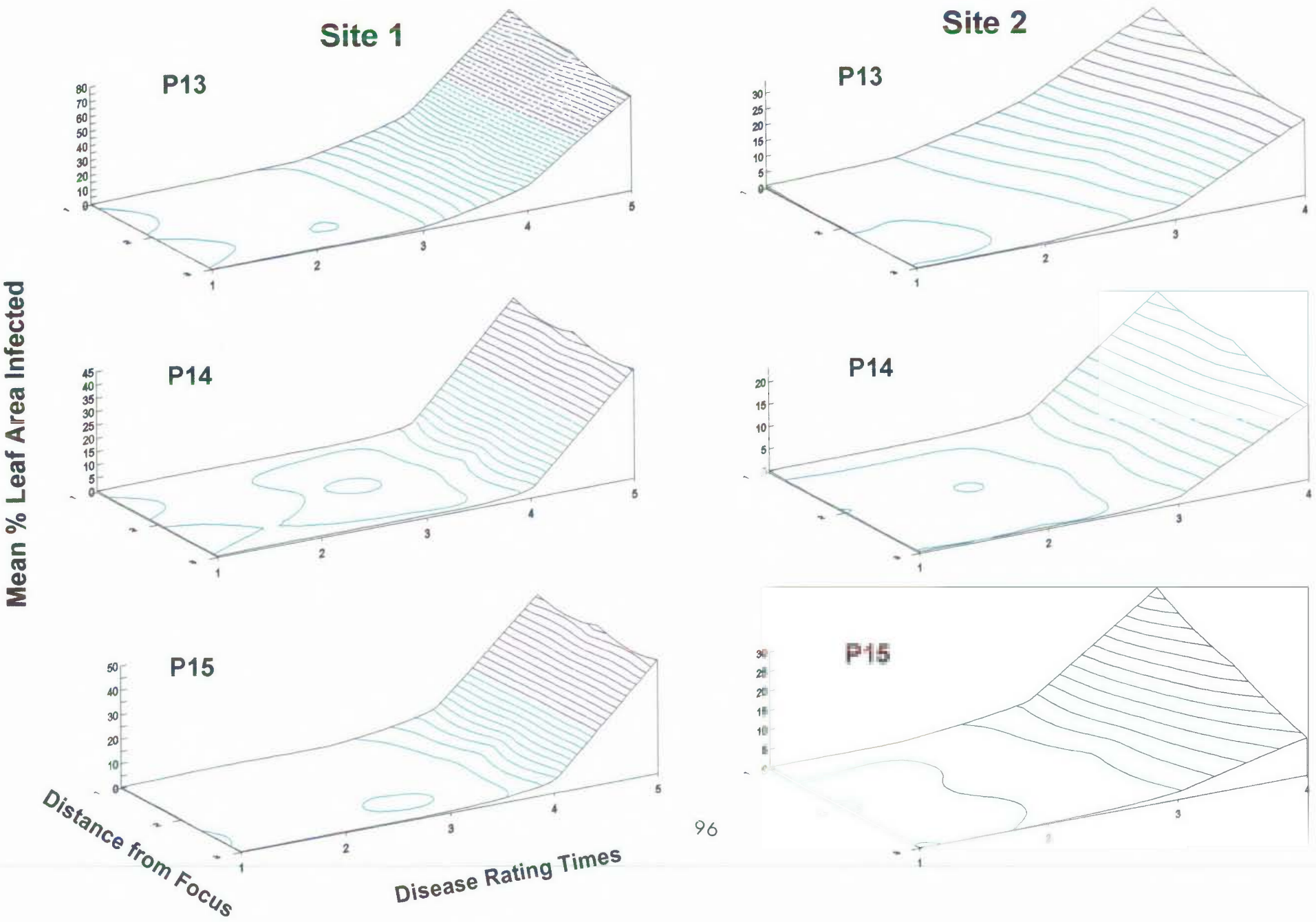
Site 1
P13
P14
P15
Site 2
P13
P14
P15
Mean % Leaf Area Infected
Distance from Focus
Disease Rating Times

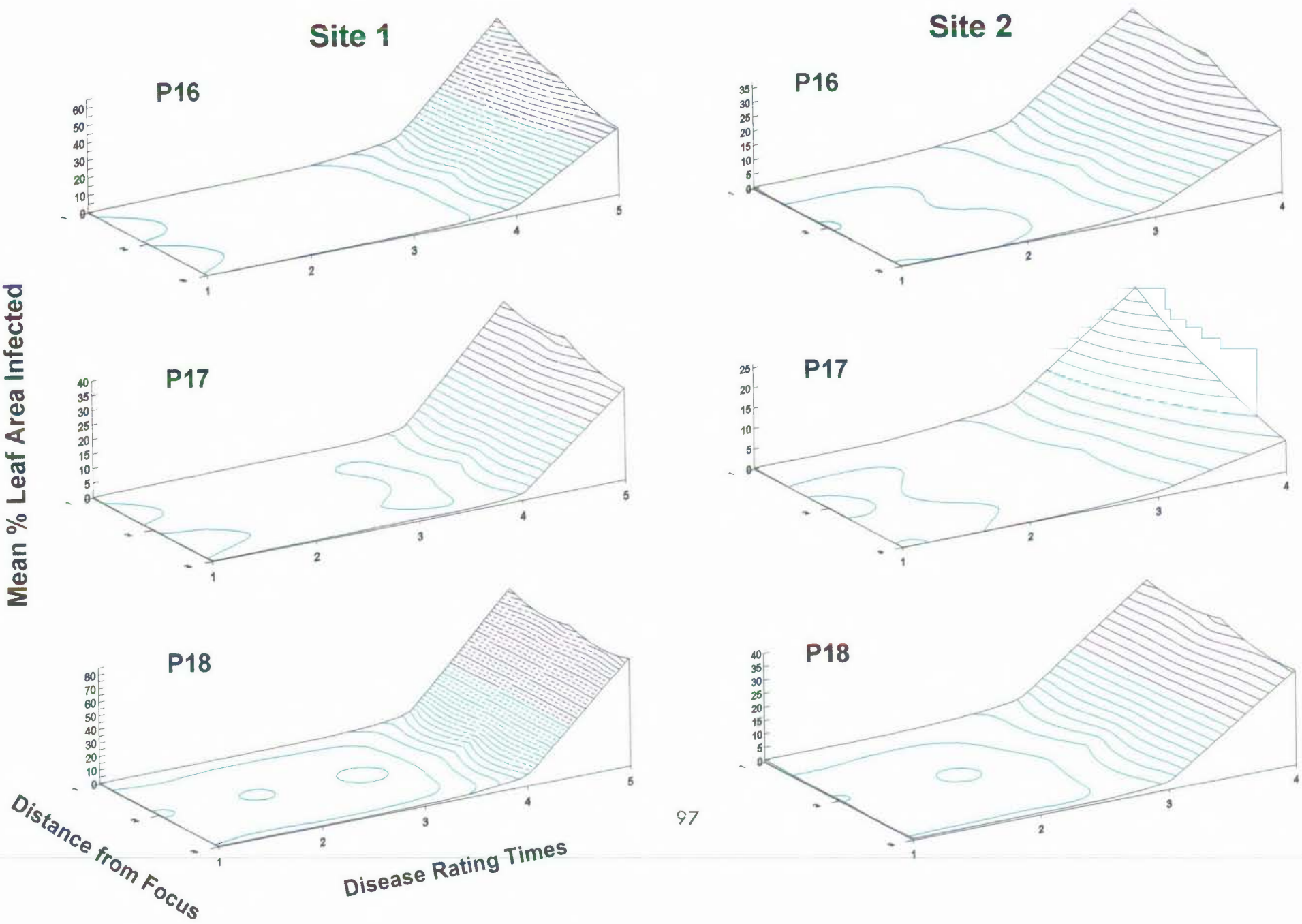
Site 1
Site 2
P16
P17
P18
Mean % Leaf Area Infected
Distance from Focus
Disease Rating Times

Figure 5.4. *Three-dimensional surface response maps showing disease progress in space and time, plotted for each sunflower line at both field sites. x axis = successive disease assessments; y axis = rows 0.8 (1), 1.6 (2) and 2.4m (3) from the focus; z axis = mean disease severity rating (% leaf area infected) for plants in each row.*

(ii) Velocity of disease spread and grid volumes

The velocities of spread (v) and grid volumes (GV) or volumes beneath the surface response maps (Figure 5.4) for the 9 sunflower lines, are shown in Table 5.9. At Site 1, the lines were separated into 4 to 6 groups, but many of these groups were overlapping. No clear trend throughout the epidemic was recognised. During the 'early' phase of the epidemic, lines P_{14} and P_{15} had the highest and lowest velocities of spread respectively. During the 'late' phase of the epidemic, line P_{18} had the highest and lines P_8 and P_9 had the lowest velocities of spread. Overall, P_{13} and P_9 had the highest and lowest velocities of spread respectively.

Table 5.9. *Spatiotemporal parameters of disease progress for 9 sunflower lines grown at two field sites. Values with the same letter are not significantly different.*

Sunflower line	Site 1				Site 2			
	[a]GV	[b]v_e	[c]v_l	[c]v_c	GV	v_e	v_l	v_c
P_1	40.62 de	0.45 bc	1.49 b	0.62 ab	17.80 e	0.21 b	0.44 b	0.23 b
P_8	63.76 c	0.37 bc	0.70 c	0.42 c	42.8 b	0.21 b	0.52 b	0.26 b
P_9	26.46 e	0.34 bc	0.58 c	0.28 d	21.93 d	0.78 b	1.02 b	1.05 b
P_{13}	112.14 a	0.50 b	1.35 b	0.74 a	54.17 a	0.18 b	0.43 b	0.25 b
P_{14}	45.86 de	0.93 a	1.67 b	0.66 ab	30.93 c	0.25 b	1.25 b	0.39 b
P_{15}	59.20 cd	0.16 c	1.50 b	0.39 cd	31.33 c	0.38 b	0.68 b	0.42 b
P_{16}	71.41 c	0.35 bc	1.82 ab	0.56 b	42.10 b	0.21 b	0.73 b	0.35 b
P_{17}	40.40 d	0.58 b	1.1 b	0.63 ab	24.75 d	0.27 b	0.48 b	0.31 b
P_{18}	90.23 b	0.24 bc	2.34 a	0.56 b	40.67 b	2.70 a	4.79 a	4.42 a

[a]GV = *Represents the grid volume or volume under the surface plot of disease progress in time and space, for the complete epidemic.*

[b]v_e = *Represents the velocity of disease spread (m/d) during the 'early' phase of the epidemic*

[c]v_l = *Represents the velocity of disease spread (m/d) during the 'late' phase of the epidemic*

[c]v_c = *Represents the velocity of disease spread (m/d) for the complete epidemic*

At Site 2, the lines were poorly separated according to their velocities of spread (Table 5.9). Only two different groups were recognised and these groups consisted of the same lines for each phase of the epidemic. One of the groups consisted of P_{18} which had the highest velocity of spread. All the other lines had the same velocities of spread.

According to their grid volumes (GV), the 9 sunflower lines were separated into 6 and 7 groups at Sites 1 and 2 respectively (Table 5.9). Some of the groups overlapped, which reduced the number of discrete groups at each site to 5. At both sites, line P_{13} had the largest GV and lines P_9 and P_1 had the smallest GV's at Sites 1 and 2 respectively.

5.4.6 Correlations between epidemic parameters

Spearman's correlation coefficients for all the epidemic parameters calculated from the data obtained at Sites 1 and 2 are shown in Tables 5.10 and 5.11 respectively. Parameters with correlation coefficients of 0.7 or greater were considered to show a high degree of rank similarity. At both sites, DSRs, audpcs and GVs were very highly correlated for all phases of the epidemic. There was also a high degree of correlation between audpcs for the various epidemic phases. DSRs for each assessment time were generally highly correlated with each other at both sites. DSRs were poorly correlated with all other parameters. At Site 1, there was was high negative correlation between velocity of spread (v) and disease gradient (b). Generally, gradients b_e, b_l and b_c were well correlated with each other at both field sites, as were velocites of spread, v_e, v_l and v_c. However, correlations between apparent infection rates (r) for each phase of the epidemics were poor at both sites.

Table 5.10. *Spearman's correlation coefficients for epidemic parameters determined from plants grown at Site 1. Parameters include area under the disease progress curve (audpc), apparent infection rate (r), disease gradient (b), velocity of disease spread (v), volume beneath the surface plot of disease progress in space and time(GV) and mean percentage leaf area infected per plant.*

	[a] Epidemic Parameters																	
	$audpc_e$	$audpc_l$	$audpc_c$	r_e	r_l	r_c	b_e	b_l	b_c	v_e	v_l	v_c	GV	[b]DSR1	DSR 2	DSR 3	DSR 4	DSR 5
$audpc_e$	1.00																	
$audpc_l$	[c]0.80	1.00																
$audpc_c$	0.80	1.00	1.00															
r_e	-0.18	-0.27	-0.27	1.00														
r_l	0.25	0.75	0.75	-0.21	1.00													
r_c	0.09	0.34	0.34	0.64	0.44	1.00												
b_e	0.23	-0.17	-0.17	0.20	-0.70	-0.10	1.00											
b_l	0.12	-0.15	-0.15	0.70	-0.42	0.33	0.47	1.00										
b_c	0.35	-0.10	-0.10	0.38	-0.63	0.03	0.85	0.77	1.00									
v_e	-0.23	-0.13	-0.13	0.33	0.24	0.05	-0.70	0.05	-0.43	1.00								
v_l	0.10	0.48	0.48	-0.78	0.64	-0.21	-0.43	-0.88	-0.70	-0.18	1.00							
v_c	0.05	0.28	0.28	-0.05	0.60	0.10	-0.85	-0.22	-0.62	0.83	0.22	1.00						
GV	0.75	0.98	0.98	-0.33	0.78	0.31	-0.22	-0.17	-0.12	-0.17	0.52	0.27	1.00					
[b]DSR1	0.73	0.74	0.74	-0.60	0.36	-0.09	0.20	-0.41	0.03	-0.61	0.61	-0.24	0.74	1.00				
DSR 2	0.93	0.70	0.70	-0.22	0.14	-0.13	0.18	0.08	0.32	-0.03	0.07	0.20	0.60	0.59	1.00			
DSR 3	0.88	0.92	0.92	-0.10	0.54	0.28	0.00	0.17	0.15	-0.05	0.18	0.23	0.88	0.62	0.78	1.00		
DSR 4	0.82	0.98	0.98	-0.30	0.70	0.23	-0.13	-0.12	-0.05	-0.10	0.47	0.30	0.97	0.72	0.73	0.93	1.00	
DSR 5	0.70	0.97	0.97	-0.37	0.80	0.33	-0.20	-0.25	-0.18	-0.25	0.60	0.18	0.98	0.78	0.50	0.83	0.93	1.00

[a] *Subscripts 'e' and 'l' represent parameter values for the 'early' and 'late' phases of epidemic development, and subscript 'c' represents the parameter values for the complete epidemic.*

[b] *DSR 1 represents disease severity at the first rating time, DSR 2 at the second rating time, ...and DSR 5 at the fifth rating time.*

[c] *Coefficients ≥ +0.7 are surrounded by a solid-line border, those ≥ -0.7.are surrounded by a dotted-line border.*

Table 5.11. *Spearman's correlation coefficients for epidemic parameters determined from plants grown at Site 2. Parameters include, area under the disease progress curve (audpc), apparent infection rate (r), disease gradient (b), velocity of disease spread (v), volume beneath the surface plot of disease progress in space and time(GV) and mean percentage leaf area infected per plant.*

	[a] Epidemic Parameters																
	$audpc_e$	$audpc_l$	$audpc_c$	r_e	r_l	r_c	b_e	b_l	b_c	v_e	v_l	v_c	GV	[b]DSR 1	DSR 2	DSR 3	DSR 4
$audpc_e$	1.00																
$audpc_l$	[c]0.83	1.00															
$audpc_c$	0.83	1.00	1.00														
r_e	-0.58	-0.66	-0.66	1.00													
r_l	-0.15	0.04	0.04	0.08	1.00												
r_c	-0.57	-0.39	-0.39	0.73	0.51	1.00											
b_e	-0.22	-0.47	-0.47	0.80	-0.41	0.33	1.00										
b_l	-0.17	-0.63	-0.63	0.61	-0.29	0.10	0.70	1.00									
b_c	-0.23	-0.49	-0.49	0.82	-0.36	0.37	1.00	0.73	1.00								
v_e	-0.42	-0.28	-0.28	0.07	0.22	0.16	-0.40	-0.05	-0.39	1.00							
v_l	-0.20	0.03	0.03	-0.02	0.60	0.47	-0.50	-0.35	-0.47	0.70	1.00						
v_c	-0.07	0.07	0.07	-0.12	0.39	0.14	-0.54	-0.25	-0.53	0.87	0.88	1.00					
GV	0.92	0.95	0.95	-0.64	0.04	-0.43	-0.36	-0.48	-0.37	-0.49	-0.10	-0.10	1.00				
[b]DSR1	0.88	0.93	0.93	-0.48	-0.05	-0.27	-0.23	-0.42	-0.27	-0.35	0.05	0.05	0.93	1.00			
DSR 2	0.92	0.92	0.92	-0.59	-0.15	-0.56	-0.33	-0.33	-0.34	-0.27	-0.17	0.00	0.90	0.88	1.00		
DSR 3	1.00	0.83	0.83	-0.58	-0.15	-0.57	-0.22	-0.17	-0.23	-0.42	-0.20	-0.07	0.92	0.88	0.92	1.00	
DSR 4	0.70	0.95	0.95	-0.73	0.15	-0.32	-0.62	-0.73	-0.64	-0.19	0.12	0.10	0.87	0.81	0.80	0.70	1.00

[a] *Subscripts e and c represent parameter values for the 'early' and 'late' phases of epidemic development, and subscript c represents the parameter values for the complete epidemic.*

[b] *DSR 1 represents disease severity at the first rating time, DSR 2 at the second rating time, ...and DSR 5 at the fifth rating time.*

[c] *Coefficients ≥ +0.7 are surrounded by a solid-line border, those ≥ -0.7.are surrounded by a dotted-line border.*

5.4.7 Determining the relationship between DSRs for different leaf positions

For Site 1, the DSRs for the low plant position were regressed with DSRs for the middle and upper plant positions. The coefficients of determination for the regressions are shown in Table 5.12. These coefficients show whether disease levels at the different plant positions are co-related and can be used for predictive purposes. For example, could disease levels at the upper plant position be used to gauge disease levels at the low plant position. For some lines, and particularly at the fourth rating time, correlation was reasonably high between the different plant positions. Overall though, correlations were inconsistent. Disease levels at the middle and upper plant positions did not readily reflect disease levels at the low plant position.

Table 5.12. *Coefficients of determination for the regressions of DSRs at the low plant position with DSRs at the middle and upper plant positions for all sunflower lines grown at Site 1.*

Sunflower line	[a]$Site1_{50}$	$Site1_{56}$	$Site1_{65}$	$Site1_{72}$	$Site1_{78}$
P_1	[b]0.70	0.00	0.19	0.83	0.32
	[c]0.00	0.07	0.11	0.72	0.25
P_2	0.15	0.14	0.56	0.57	0.60
	0.00	0.07	0.31	0.33	0.34
P_3	0.25	0.07	0.19	0.80	0.32
	0.00	0.04	0.04	0.76	0.17
P_5	0.67	0.51	0.72	0.72	0.56
	0.18	0.50	0.75	0.72	0.15
P_6	0.80	0.02	0.12	0.88	0.40
	0.71	0.02	0.09	0.65	0.38
P_7	0.54	0.00	0.14	0.77	0.00
	0.00	0.31	0.10	0.62	0.00
P_8	0.01	0.12	0.07	0.71	0.20
	0.34	0.00	0.00	0.81	0.10
P_9	0.39	0.09	0.40	0.66	0.20
	0.00	0.07	0.09	0.65	0.10
P_{10}	0.62	0.16	0.02	0.76	0.10
	0.03	0.00	0.00	0.44	0.14

[a] *Subscripts refer to the number of days after planting.*

[b] *Refers to the coefficient of determination for the regression of DSR for the low plant position with DSR for the middle plant position.*

[c] *Refers to the coefficient of determination for the regression of DSR for the low plant position with DSR for the upper plant position*

5.5 Discussion

The progress of epidemics caused by *A. helianthi* followed a similar pattern in all the sunflower lines tested at both field sites. This pattern was of two distinct epidemic phases, simply referred to as the 'early' and 'late' phases. The different phases of each epidemic were analysed separately because of the large differences in disease intensity between these phases. Separate analyses would discern epidemic characteristics that might be masked by modeling the entire epidemic over time. For example, changes in the expression of QR in the various sunflower lines with increasing disease intensity could be detected in separate analyses. The 'early' phase of each epidemic was characterised by low apparent infection rates (r), disease severity ratings (DSRs) and audpcs. In contrast, the 'late' phase had high apparent infection rates and large DSRs and audpcs. In general, disease gradients (b) were steeper during the early phase for most sunflower lines. Velocities of spread (v) calculated as r/b were consequently slower during the 'early' phase at both sites.

This 'lag' then 'explode' pattern is typical of *A. helianthi* epidemics in Australia, particularly in regions where sunflower crops mature during the monsoonal period of mid- to late- summer. Temperatures above 25°C and extended periods of wet weather at flowering, favour the development of *A. helianthi* epidemics (Allen *et al.*, 1983a;b). Unless there is frequent rainfall, disease increase during the early stages of plant development is typically slow. At the Gatton site, approximately 400mm of water was applied through an overhead misting system, over a period of 23 days from the time of inoculation. Each misting schedule lasted from 4-6h. Despite this, epidemic development was slow. In a review of 77 epidemics caused by *Alternaria* pathogens, Rotem (1994) concluded that overhead misting systems contributed little to the development of alternaria epidemics compared with dew and rainfall. He also pointed out that many crop plants have increased resistance to *Alternaria* pathogens during their juvenile growth phase, which may further contribute to slow epidemic development.

The factors which would lead to this type of epidemic pattern occurred at the two field sites used in this study. Average daily temperatures at both sites were favourable for disease development and at flowering, overcast wet conditions prevailed. The dependence *A. helianthi* has for long periods of free moisture on leaves was illustrated at Site 1, where disease severity increased rapidly following 9 consecutive days of wet weather during flowering. In contrast, the increase in disease intensity at Site 2 was much lower, following a wet period of only 2 or 3 days. This requirement for long, wet periods is limiting for the pathogen and thus restricts its importance to seasons when these conditions prevail.

Linearisation of disease progress curves is a prerequisite to epidemic analysis. The reduction of disease progress to mathematical functions based on linear relationships is essential for the purposes of comparing epidemics. However, there is no simple rule of thumb for choosing an appropriate transformation model (Waggoner, 1986), and each model must be tested on a case by case basis. In this study, the logistic model best described epidemic progress as indicated by the coefficients of determination (R^2) obtained from the linear regressions of disease severity with time. The reason that the logistic gave a better fit than the Gompertz model may have been due to the overall epidemic pattern, characterised by a long 'lag' phase in which disease levels were very low, followed by a short phase of rapid disease increase. Waggoner (1986) found that in general, the logistic model more closely fit such negatively skewed progress curves. Headrick and Pataky (1988) concluded that logistic models better describe diseases in which susceptability of the host increases with age and that Gompertz models fit those diseases characterised by adult plant resistance. Their observations confirm Waggoner's (1986) findings relating to skewness at a more fundamental level and are supported by the epidemic patterns shown by *A. helianthi* in this study.

The parameter disease severity rating (DSR), determined as an estimate of the percentage leaf area infected per plant, was considered to be the most direct indicator of a plants'

resistance to *A. helianthi*. Using DSR, good correlations were obtained for the rankings of the 9 sunflower lines over locations and to a lesser extent, years. The relative value of other epidemic parameters in differentiating QR was therefore determined by their degree of correlation with the DSR. Coefficients based on Spearman's ranking were used as a measure of correlation between parameters.

For both sites, correlations between DSRs and other epidemic parameters were poor. That is, the the rank order of the lines for each epidemic parameter was not well correlated with the order of lines ranked by DSRs. This suggests that parameters other than the DSR do not differentiate lines according to their level of resistance. The reason for this lack of correlation may be that parameters such as apparent infection rate (r) and disease gradient (b) provide no information about disease severity as such, but instead only give an indication of the magnitude of change between points on a regression line. This means that a sunflower plant that undergoes a two or three-fold increase in disease over a specified time will have a high value for r , but this relative increase may be at a very low level of disease. For example, at both field sites, the line P_9 had the highest apparent infection rate during the 'early' phase of the epidemic and the lowest DSR. This was because during this phase, the relative increase in disease was high but overall, it began and ended at an extremely low level of disease. Therefore, parameters based on regressions which do not reflect actual disease levels cannot be used for comparative purposes when selecting lines with QR. This problem can be compensated for to some extent if regression lines are forced through the origin, thereby giving all regressions the same starting point. However, this practice can severely compromise the accuracy of the regression line (R^2) and consequently, r. The use of apparent infection rate for differentiating partial or quantitative resistance has been questioned by Luke and Berger (1982), Shaner and Finney (1977) and Wilcoxson *et al.*(1975), however their criticisms were largely aimed at the use of logits, which tend to amplify differences in severity at low levels of infection.

Similarly, the magnitude of disease gradients can be misleading, and should not be relied upon to compare QR among sunflower lines. In assessing slow-rusting of oats, Luke and Berger (1982) found that isopathic rates gave a reliable method of differentiating oat cultivars, but found that disease gradients and final disease (Y_{max}) were less reliable. Mackenzie (1975) and Headrick and Pataky (1988) also considered disease gradients to be poor indicators of partial resistance.

Velocities of spread, calculated from the regression-derived parameters *r* and *b*, likewise suffer from an inability to discern actual levels of disease and were also poorly correlated with DSRs. Furthermore, since *r* and *b* are estimates of linear functions, the accuracy of *v* is dependent to some degree on the accuracy of their estimation. There is therefore, considerable scope for errors to be compounded in this calculation. Van der Bosch *et al.* (1988) found that the velocity of disease spread may be erratic during the early generations of epidemics caused by polycyclic diseases. This may be partly due to continuous changes in disease gradients due to the waveform pattern of disease spread (Minogue, 1986; Ferradino, 1993). Minogue and Fry (1983) warned that a large scale of observation may be required to take full account of this wave. In this regard, the plot size used in these field experiments may have been too small to adequately measure velocities of spread.

It was found that parameters that reflect actual disease levels, such as audpc and grid volumes (GV), were highly correlated with DSR. Audpc is widely used in plant pathology for analysing epidemics in fungicide and resistance trials. Both Shaner and Finney (1977) and Fry (1978) found it to be a better measure of treatment differences than *r*, because it uses actual rather than transformed severity data and it reflects 'both the onset and rate of epidemic development". From an examination of eight epidemiological parameters used to characterise partial resistance to anthracnose in *S. scabra*, Chakraborty *et al.* (1990) found that audpc was the best measure of resistance. Mehdi, Carson and Lay (1984) used audpc to determine phenotypic and genotypic correlations for reaction to *A. helianthi* in suflower. Later, Carson (1985b) used DSRs to evaluate inbred sunflower

lines for resistance to *A. helianthi.* The audpc represents the integral of the percentages *x* of diseased leaf tissue over time and thus incorporates fluctuations in time not represented in a single disease rating. For this reason, it may be a more useful indicator of QR than the DSR taken at a critical point.

The grid volume (GV) is a measure of the volume beneath the surface plot of disease progress in time and space. It has the potential of being a more accurate measure of disease than audpc because it accounts for disease in three dimensions, taking in fluctuations that are 'smoothed out' in the estimation of two-dimensional audpc. To the authors' knowledge, GV is not commonly used as an epidemic parameter, although surface response maps have been used in conjunction with infection and/or isopathic rates to differentiate partial resistance of sweet corn to common rust (Headrick and Pataky 1988).

Audpcs for the 'early' and 'late' epidemic phases were highly correlated, as were the DSRs for each rating time, at both field sites. This indicates that these parameters are robust and adequately reflect QR under conditions of increasing plant age and disease intensity. This suggests that selections can be made with a high degree of confidence prior to flowering, thereby saving much time and effort. If selection is delayed until late- or post- flowering, as would occur if the critical point model (Allen,1981) were used, a large proportion of plants must be 'bagged' to the ensure that at least some resistant plants were available for controlled pollination.

As mentioned previously, the value of epidemic parameters in evaluating QR depended primarily on their correlation with DSRs. The ability of the parameters to separate lines for QR was a secondary but essential criterion in their evaluation. Values for audpc, GV and DSR provided a high degree of separation among the sunflower lines evaluated. Indeed, those parameters that gave low or negative correlation coefficients with DSR also gave poor separation of the sunflower lines. Generally, there was less separation of the lines at low levels of disease, such as during the early phase of the epidemic. Also, fewer groupings

were differentiated at Site 2, where there was a lower overall disease severity. Because the 'late' phase of each epidemic contributed such a large proportion to the complete epidemic, separation of lines for the 'late' phase closely resembled those of the complete epidemic.

According to the DSR, audpc and GV, the sunflower line P_{13} had the greatest susceptability to *A. helianthi*. This line was chosen as the susceptible standard for these experiments. The line P_{18} was on average, the next most susceptible line but at Site 2, had considerably more disease than P_{13} at the last rating time. Lines P_1, P_9 and P_{17} were the most resistant lines, followed by the commercial hybrid, Hysun 45 CQ (P_{14}). P_9 also had the steepest disease gradients. The fact that P_9 matured later than all other lines may account for its apparent high level of resistance. Such differences in maturity between lines is a major confounding problem in the evaluation of QR (Parlevliet, 1986, Wolfe and Gessler, 1992) and one that can only be resolved through repeated testing (Simmonds, 1991). Despite a relatively fast rate of maturity, line P_{17} maintained a high level of resistance. This line was observed to have a very open leaf habit, which may have contributed to its' resistance. Plant architecture is known to affect microclimate close to the infection court (Burdon, 1982) which in turn can influence disease development. Both plant stature and density have been shown to greatly influence infection of sunflower by *A. helianthi* (Carson, 1986).

Three-dimensional surface response maps were obtained by plotting the DSRs (z axis) for each plant in a plot against time (x axis) and distance (y axis) from the disease focus. The resulting surface response maps allowed the epidemics for each line to be viewed in both space and time. These maps provide a useful way to conceptualise the response of each line to increasing amounts of infection and may therefore help to evaluate resistance in a way not offered by the parameters separately. Contour lines on each map represent isopaths, connecting points of equal disease. Essentially, isopath movement in space and time can be viewed on the surface plot. A quick estimate of the isopathic rates as proposed by Berger and Luke (1979), can be obtained from the maps. They are determined as the relative position of isopaths as they they move in space (yaxis) and time (x axis). That is, the

difference in their starting and finishing positions as they cross the x axis, giving a rate of movement in md^{-1}. For example, late in the epidemic, isopathic rates were generally much higher at Site 1 than at Site 2.

Disease gradients and their effect on isopath movement are clearly indicated on the maps. Generally, steep disease gradients indicate slow isopathic rates. Exceptions to this trend were shown at Site 1 by P_{13} and P_{16}, whose disease gradients remained relatively steep, despite very high levels of disease. This may have been due to a rapid increase in disease levels at the focus, particularly on leaves at the top of the plants. Disease gradients at Site 2 were steeper than at Site 1, due to a slower rate of spread from low levels of disease. Disease spread was slowest in line P_9 at both field sites. Overall, disease gradients (*b*) tended to flatten over time (Table 5.8), however this is not shown on the maps as the scale cannot discern the extremely low levels of disease present during the early stages of the epidemics. Flattening of disease gradients with time is commonly due to the effect of secondary spread of inoculum (Gregory,1968) or because of a limitation of infection sites (Aylor and Ferrandino, 1989). The first of these is likely to account for the observations found in this study.

Rates of disease progress are indicated on the maps as the distance between isopaths. For example, at both sites, the isopaths for P_{13}, P_{16} and P_{18} were close together indicating a fast rate of disease increase, while those of P_9 were far apart indicating a slower rate of disease increase. With the exception of the susceptible line P_{13}, disease progress increased dramatically in all lines at the same point in time, indicating the strong interaction between plant age and favourable weather conditions. Epidemic development began sooner in P_{13} than in all other lines. Its rate of disease increase therefore appears less dramatic at the point of transition even though it reached a high level of infection.

As was indicated by the calculated *r* (Table 5.6), the maps also show that there was relatively little difference in rates of disease progress between the various sunflower lines, despite there being large differences in their DSRs. This suggests that disease increased

at a constant rate regardless of the amount of diseased tissue on each line. This is contrary to expectation. Disease normally increases at a proportional (exponentional) rate. Lines with high levels of disease would be expected to have faster rates of infection than those with low levels. This anomaly may be partly due to the effect of the logarithmic transformation used to linearise progress curves. This transformation tends to "severely" amplify differences at the bottom end of the scale of measurement (Gilbert, 1989). This would tend to unduly increase the slope of the regression line when fitted to extremely low levels of disease. Highly resistant sunflower lines would then have inflated *r* values.

The process of rating individual leaf pairs on individual plants is tedious and time consuming. Infection on the lower leaves of plants is a good indicator of resistance, since *A. helianthi* infections typically spread up the plant from the oldest, to progressively aging, plant tissue. In a mature sunflower crop, the assessment of leaves in the lower canopy can be quite arduous. If disease levels higher up on the plant could be used to assess QR then the rating process could be made easier. The predictive value of disease on leaves in the middle and upper parts of the plant was assessed by multiple regression of the DSRs' for leaves in each position. The resulting regression coefficients indicated that in general, the DSRs' on the lower leaves could not be predicted by those on leaves in the middle and upper plant positions. This suggests that the rate of disease increase up the plant is not linear. This may be due to both the environmental conditions that either favour or retard disease development and/or the rate at which tissue becomes more susceptible to infection (growth stage). Late in the epidemic at Site 1, disease on the middle and upper leaves gave reasonable predictions of disease on the lower leaves in 6 of the 9 lines. However, this level of prediction declined thereafter. Infection probably follows patterns of 'lag' and 'explosion' within each plant, where disease levels increase to a high level on any one leaf while the succeeding leaf pair is still in 'lag'. This effect would tend to diminish late in the epidemic, which may explain why disease ratings taken at late anthesis provide reliable estimates of resistance.

The results arising from this study indicate that DSRs, audpcs and grid volumes can be used prior to flowering to differentiate sunflower lines expressing QR to *A. helianthi.* However, it must be recognised that this conclusion is based on a limited study, in which a single epidemic pattern was evident. Whether these parameters could be used for other types of epidemic patterns is unknown. Parameters such as apparent infection rate and disease gradients, although unsuitable comparative indicators of QR, may be of use when examining epidemic patterns in specific sunflower lines. Three-dimensional surface response maps were useful for visualising epidemics in both space and time, allowing isopathic rates, infection rates, disease gradients and severity, to be viewed simultaneously. The data obtained from this study provided a pool of information against which the greenhouse screening assay was tested (Chapter 7).